

Mechanical properties hysteresis of unsaturated granular soil

Paul Chiasson^{1*}, and Horace Tamégnon²

¹Département de génie civil, Université de Moncton, Moncton, NB E1A 3E9, Canada

²ECOGEC SARL, Lot No. 36-E boulevard Steinmetz Saint-Michel, Cotonou, Benin

Abstract. The soil-water characteristic curve reveals that the studied very dense crushed sand and gravel proves unable to maintain a saturated state under a positive matric suction. Capillary physics explains how this could result from the presence of millimetre size pores. An innovative pendular model gives insight on why consolidated drained triaxial tests give higher mechanical properties after drying followed by wetting than after drying alone. The model shows how particle tilting induced by shearing may squeeze pendular water into the funicular regime and provoke drainage as observed during both contraction and dilation phases. It also highlights that particle tilting produces changes of matric suction within pendular water and why dilation increases with applied matric suction while confinement stress yields the opposite.

1 Introduction

The hysteresis of the water content of unsaturated soils, where at a same matric suction, the water content in the drying phase exceeds that during wetting, is a well-known phenomenon. It affects engineering properties such as the hydraulic conductivity, but certain studies also highlight shear strength. According to CD tests (triaxial or direct shear), some researchers such as [1] find for both a silt and a kaolin a slightly higher shear strength after drying than after a drying and wetting cycle. Others, such as [2] report the opposite for a manufactured silt. Research on hysteresis of mechanical properties appears concentrated on fine-grained soils or containing high proportions of fine particles (often plastic). Little has been published on coarse-grained soils although of common use in civil engineering, including in capillary barriers.

This study aims to evaluate the influence of hysteresis of the water retention curve on mechanical properties. It first investigates the degree of saturation during drying and subsequent wetting. It follows with mechanical properties as measured using triaxial CD tests after desorption alone and after a desorption-sorption cycle. It finally develops a pendular model to give some insight on the shearing behaviour of the material.

2 Testing Program

The studied material consists of a crushed sand and gravel with traces of silt from the Moncton Crush Stone Quarry (NB, Canada). It contains 8.9% non-plastic fines, 66.0% sand, 25.1% fine gravel with 2.7 mm for median grain size (D_{50}) and an effective size (D_{10}) of 0.10 mm. Coefficients of curvature and of uniformity are respectively of 5.9 and 35, giving a SW-SM. All specimens of this study are prepared at optimum standard Proctor (dry density of

2,100 kg/m³ and 7% water content). Two specimen variants were prepared and are later discussed (Fig. 1).

Shear strength testing in an unsaturated state proceeded in a modified Bishop and Wesley triaxial cell. Specimen preparation includes manufacturing specimens through successive static compaction of five (5) 20 mm layers in a 50 mm diameter mould (Fig. 1b). These are set on a 300 kPa high air-entry value porous stone embedded in a pedestal and topped by a coarse-grained porous stone. Saturation proceeds with de-aired distilled water until completed, that is after reaching a Skempton coefficient (B) of 0.97 [3]. Consolidation then follows under a predefined confinement stress.

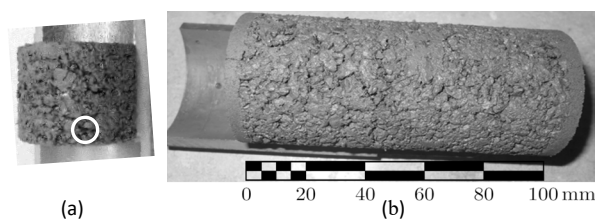


Fig 1. Statically compacted specimens used for (a) measurement of soil-water retention and (b) triaxial shear. The circled void at left has an approximate width of 6.3 mm.

Desorption begins by applying air pressure (u_a) at the top end equal to the water back pressure (u_w) applied at the base. Subsequently decreasing the latter creates a matric suction ($u_a - u_w$) that dries the specimen by water drainage through the base. The desorption-sorption cycle requires a prior desorption step at a suction of 295 kPa. Following this, increasing the water pressure to a target value lowers the suction and induces water to flow back into the specimen (wetting). During the desaturation operation called the equilibrium phase, the isotropic confinement pressure in the cell remains unchanged, hence maintaining the net confinement stress ($\sigma_3 - u_a$) constant with positive air and water pressures.

* Corresponding author: paul.a.chiasson@umoncton.ca

Drained shearing under axial loading progressed at a constant strain rate of 0.01 mm/min up to 15% total axial strain. Unsaturated CD triaxial tests proceed under constant matric suction ($u_a - u_w$) and constant net confining stress ($\sigma_3 - u_a$). Generated pore water and pore air pressures from shearing are dissipated by drainage by the base (water) and top end (air) of the specimen.

Measurements of the soil-water characteristic curve (SWCC) above 5 kPa of matric suction proceeded in the modified triaxial apparatus by the axis-translation technique with 100 kPa of net cell pressure ($\sigma_3 - u_a$). The 50 mm diameter specimen had a reduced height of 40 mm (Fig. 1a) to minimize time for water content equilibrium.

Column tests allow applying matric suctions between 0.10 and 1.0 kPa with little error. Material static compaction proceeded in a steel tube by a succession of 20 mm layers up to a total height of 120 mm. Drying tests start by saturating the column under vacuum in an air- and water-tight cell and a slow water inflow from the base. Once saturation confirmed by reaching the targeted total mass, cell and specimen were then let to drain by the base soaking in water. Columns tests were extended up to 47 days to stabilize within 0.1 g of total setup mass, ensuring an error below 0.2% in degree of saturation.

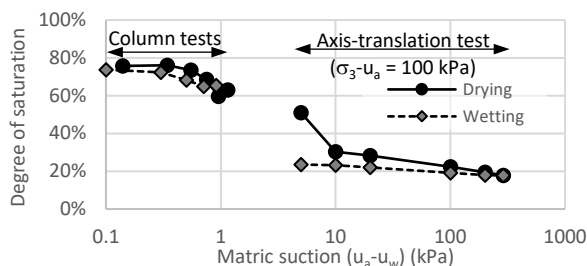


Fig. 2. SWCC from column tests ($\sigma_3 - u_a = 0$ kPa) and axis-translation technique in the triaxial cell ($\sigma_3 - u_a = 100$ kPa).

In desorption, column tests immediately reveal an unsaturated state at a matric suction of 0.14 kPa (Fig. 2). This 14 mm total water head corresponds to one of the smallest matric suctions achievable by this method that allows a reliable measurement of water content on a representative volume. Exerting a lower suction would require a thinner specimen. For example, a layer of 2 mm in thickness touching water at its base yields a matric suction of 0.01 kPa at mid-height. Given the material grain sizes (and pores), this wouldn't create a representative volume. Hence, physics and specimen representativeness impose a minimum limit to matric suction. To name a few, this statement applies to tests performed in columns and by the axis-translation technique in Tempe or triaxial cells.

The studied soil maintains approximately 74% saturation for the two subsequent measurements (Fig. 2). It then dries up abruptly beyond 0.55 kPa of matric suction at a desaturation gradient of 25.3%/kPa.

Tests in the triaxial cell by the axis-translation technique were carried out under a net confinement stress which is known to increase the air-entry value of unsaturated soils [4]. These latter measurements will therefore move to the right compared to those from column tests. This could explain a certain discontinuity in the data of the two methods as presented in Fig. 2. Results

show that the degree of saturation continues to drop abruptly, reaching a residual value of about 30% at roughly 10 kPa of suction. It then decreases at a low rate to attain 17.8% at 290 kPa of matric suction. During subsequent sorption (wetting), the material absorbs water at an even lower gradient (Fig. 2) up to a water-entry value of approximately 3 to 4 kPa (300 to 400 mm of water head) at a degree of saturation in the order of 23.5%. According to column tests, the soil returns to the degree of saturation of the desorption curve at 0.1 kPa.

Between matric suctions of 0.14 to 0.55 kPa, it is interesting to observe that water content in desorption columns rest on a sill below 100% saturation. In other words, certain pores of the tested specimen cannot retain water to maintain a degree of saturation above 74%. Although this observation appears to have never been reported, close inspection of data from [5] shows a sill at a degree of saturation of 92% for a similar material with 10% non-plastic fine content. In a capillary tube, the calculation of the height of ascent h commonly uses Jurin's Law with a zero-degree contact angle. This law has, however, its limits of applicability. Moving away from the wall of a large diameter tube, gravity takes over surface tension, and the contractile skin flattens. According to a correction proposed by [6], water will only fill a tube of the same height as its capillary rise if its diameter is less than 5.1 mm. To maintain a soil saturated by capillarity, the size of all its pores must therefore fall well under 5.1 mm. That said, capillarity cannot fill a pore of this size located 5.1 mm above the free surface. Soil pores are also not tubes of circular cross-section. They are rather irregular by nature. In addition, [7] report that the shape of the contractile skin of water in soils proves much more intricate than the regular concave surface observed in a capillary tube. The relationship between the average radius of curvature of the contractile skin and the pore size of a soil certainly differs in complexity than that of the diameter of a capillary tube. As a result, the size of a pore capable of retaining saturation by capillarity would be smaller than for a capillary tube of height h equal to its diameter d . Hence, capillary rise alone cannot fill soil pores of millimetre size such as present in the tested specimens. It may be argued that soils with sufficiently large voids will present a null air-entry value.

For the tested soil specimens, the matric suction of 0.55 kPa (Fig. 2) likely defines a boundary where the larger pores cannot maintain a greater degree of saturation by capillarity (the height of capillary rise is less than their size). These pores would contain little water while smaller ones would prove completely full. None of these larger pores, however, could preserve a greater water content at smaller suctions. In these, gravity would widely take over surface tension and the water content would be limited to that around the points of contact and as thin films.

Close inspection of the surface of specimens shows the existence of pores up to 6 mm in width (Fig. 1a). Arching of larger particles against the steel mould during sample preparation is believed to have caused their presence. As discussed earlier, it is highly likely that these large pores cannot saturate by capillarity. It hence appears that the tested specimens feature a null air-entry value. They may remain in the saturated state only if $(u_a - u_w) \leq 0$.

In other words, when water reaches a pressure greater than or equal to that of the air (as below the free surface).

3 Mechanical Properties

Mechanical properties in the saturated state such as the failure criterion and the volume change during shearing were investigated through consolidated drained triaxial tests. As expected, the material behaves under loading as a dense granular soil. The failure envelope reveals zero effective cohesion and a 43.6° angle of internal friction.

Shearing action in the unsaturated state on the drying path was investigated through 15 CD triaxial tests conducted at matric suctions of 5 to 290 kPa under net confinements ranging from 100 to 250 kPa. Of these, five were performed at a constant net confinement of 100 kPa and matric suctions of 5 to 290 kPa (Fig. 3 presents typical results). These aim to evaluate the effect of matric suction alone on the mechanical behaviour in drained loading.

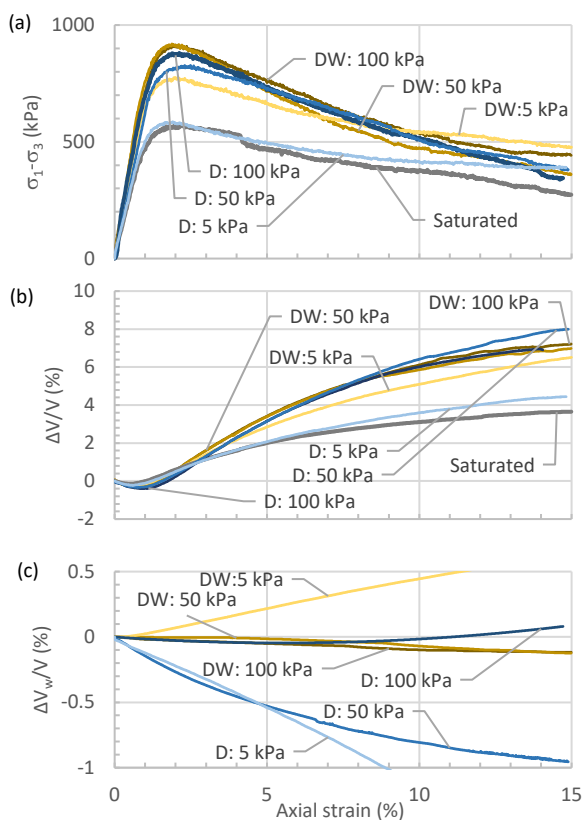


Fig 3. A subset of saturated and unsaturated triaxial tests: (a) principal stress difference; (b) volumetric strain; (c) change in volumetric water content.

Shearing produces total volume changes with initial contraction followed by expansion (Fig. 3b). For the first 0.5% to 1% axial strain, the volume of voids of the unsaturated soil decreases faster than that of water in the pores (Fig. 3). Consequently, the degree of saturation rises slightly (Fig. 4). This occurs in the elastic stage where the specimen exhibits low plastic strain (little rearrangement of the grains). Beyond 1% of axial strain, the degree of saturation diminishes (Fig. 4). Above 7% axial strain, the rate of change in the degree of saturation declines, a sign that the material tends towards a state of

equilibrium even if it continues to deform. Similarly, so does the rate of volume change (Fig. 3b).

Changes in total and water volume hence draw a path of the degree of saturation versus matric suction (Fig. 4). The SWCC first moves slightly upwards and then downward, passing through its value at peak shear strength and pursuing asymptotically towards a minimum. Shear thus creates a set of characteristic curves. As shown by Fig. 4, a drained test at constant matric suction does not imply a constant degree of saturation during shear. This is worthwhile noting.

Another interesting feature arises while shearing on the drying path. Water drains constantly during the test (Fig.3c), even throughout the dilation phase. The latter appears contradictory and is investigated in the following discussion.

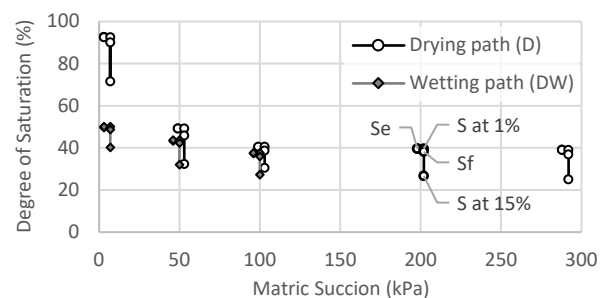


Fig. 4. Degree of saturation during unsaturated shear ($\sigma_3 - u_a = 100$ kPa). S_e , S at 1%, S_f and S at 15% are at equilibrium, 1% axial strain, failure and 15% axial strain. Tick marks are slightly offset from true values to show the path followed.

Fredlund et al.'s [8] defined the extended Mohr-Coulomb failure criterion for unsaturated soils as:

$$\tau_{ff} = c' + (\sigma_{ff} - u_{af}) \tan \phi' + (u_a - u_w)_f \tan \phi^b \quad (1)$$

where c' , $(\sigma_{ff} - u_{af})$, ϕ' , $(u_a - u_w)_f$ and ϕ^b represent effective cohesion, net normal stress on the failure plane at failure, angle of internal friction, matric suction at failure and angle of the rate of increase in shear strength due to matric suction. Test data on the drying path for capillary cohesion (third term on the right) as defined by:

$$c_{cap} = (u_a - u_w)_f \tan \phi^b \quad (2)$$

indicates it increases up to a matric suction of 200 kPa and appears to diminish beyond (Fig. 5). Equation (2) provides good predictions for $\phi^b = 42.5^\circ$ under 50 kPa of matric suction. Beyond, the angle ϕ^b decreases, and the following gives better results:

$$c_{cap} = 0.9171(u_a - u_w)_f - 0.0021((u_a - u_w)_f)^2 \quad (3)$$

Mechanical properties of the studied soil were also investigated after a preliminary desorption-sorption path. This path follows in order: saturation, consolidation under confinement stress, drying under a matric suction of 295 kPa and wetting by decreasing the matric suction to a target value. Shearing proceeded through three (3) triaxial CD tests at set matric suctions of 5, 50 and 100 kPa under a constant net confinement stress of 100 kPa.

On the desorption-sorption trajectory (DW in Fig. 3), the studied soil shares several behaviours observed in saturated and unsaturated desorption tests. As for unsaturated triaxial tests on the drying path (D in Fig. 3), the material after sorption shows a similar evolution in the degree of saturation during shearing (Fig. 4). However,

the degrees of saturation at failure turn out lower than those after drying alone. The primary distinction lies in a minute adjustment in volumetric water content relatively to desorption path tests (Fig. 3c). Total volume change (DW in Fig. 3b) therefore constitutes the main cause of the variation in the degree of saturation (Fig. 4).

Reducing the applied matric suction on the desorption-sorption path gradually shifts from water expulsion to absorption (Fig. 3c). For sorption under high matric suction, shearing leads to a continuous, although very low, water drainage. However, this decreases with matric suction to even reverse into water absorption. It also approaches to null for a wetting suction of 50 kPa at axial strains of less than 4.5%.

4 Discussion

Unsaturated triaxial tests performed in desorption show that matric suction leads to an increase in peak shear resistance as predicted by the equation proposed by [8]. However, as reported by [9], the relationship becomes non-linear when matric suction rises (equations (1), (3) and Fig.5). Beyond the 200 kPa drying matric suction, peak shear strength slightly diminishes. According [9], [10], the point at which shear strength begins to decrease with increased suction corresponds to that of a change of water regime of the characteristic curve. Triaxial tests thus proceeded either in the transition or residual zone. In the former, the volume of capillary water mainly rests in the funicular (interconnected) regime. In the later, pore water is in the pendular regime where it has mostly withdrawn into isolated water bridges at grain contact points.

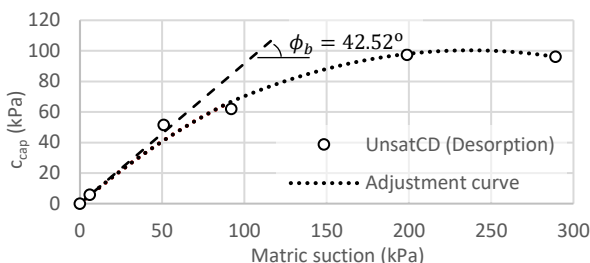


Fig. 5. Capillary cohesion c_{cap} versus matric suction for unsaturated CD tests on the desorption path (drying).

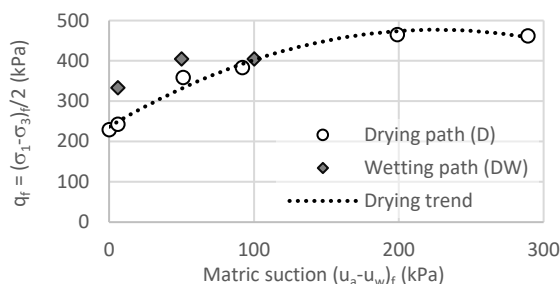


Fig. 6. Maximum shear stress at failure in function of $(u_a - u_w)_f$ for CD triaxial tests after desorption only (drying path) and after desorption and sorption (wetting path); $(\sigma_3 - u_a)_f = 100$ kPa.

In comparison to unsaturated triaxial CD tests performed after desorption, those after desorption-sorption reveal higher shear strength (Fig. 6) for a lower degree of saturation (Fig. 7). Properties such as Young's

modulus (not presented) and angle of dilation (Fig. 8) lead to identical observations. Thus, with the hysteresis of the degree of saturation (Fig. 7) comes a hysteresis effect of mechanical properties. This finding suggests that proper modelling of this material would require considering not only state variables (matric suction and net stress), but also the water content path.

The characteristic curves of Fig. 2 and 7 indicate that the column and axis-translation tests do not give the same results as those derived from the triaxial tests. These differences may find an explanation in the method of preparation of the test specimens. Examination of their photos (as earlier discussed) reveals the presence of large voids on their surface (Fig. 1).

Changes proved necessary to sample preparation after observing fissures on the high air-entry porous stone on the base pedestal following a preliminary triaxial loading of the testing program. The addition at the top and bottom of 5 mm thick soil layers composed of fine particles fixed this problem. Inspection of photos of the modified specimens indicates that this change in sample preparation also led to the elimination of large voids at both extremities (Fig. 1b). Examination of the specimens after applying confinement stress in the triaxial cell further showed that the membrane clung to their perimeter surface, closing the larger voids. This would imply greater water retention for triaxial samples. This may explain the differences between results reported in Fig. 2 and 7.

Test specimens used for triaxial testing display an air-entry value of the order of a few kPa and a water-entry value below 5 kPa (Fig. 7). Considering the steep desaturation gradient observed on samples in column tests (Fig. 2) that is typical of sands [9], residual suction of triaxial specimens should be under 50 kPa (see adjusted Brooks and Corey curve of Fig. 7).

The desorption-sorption triaxial measurements merit a last look in regards of the SWCC of the tested specimens (Fig. 7). On the desorption-sorption path, decreasing the matric suction also reduces drainage volume during shear, even reversing into continuous water absorption at the lowest tested matric suction of 5 kPa (Fig. 3). This latter test rests at a suction close to the water-entry value (Fig. 7). It hence appears that as the wetting suction approaches the water-entry value, the more the shear tendency to produce water expulsion (drainage) diminishes and to even turn into a water absorption in its vicinity.

The higher shear strength and Young's modulus observed on the desorption-sorption path compared to those on the desorption path initially appear counterintuitive. Suction stress (the combined effect of negative pore water pressure and surface tension) produces a force that pulls the grains towards one another. At the macroscopic scale, suction stress increases mobilizable friction. For a water bridge at the point of contact of two angular particles, the resultant of suction stress translates into the sum of the resultant of surface tension along the perimeter of the annular section of the pendular water and the resultant exerted by the negative water pressure (Fig. 9c). As the degree of saturation diminishes so should the size of the water bridge. Hence, at a given matric suction, the grain-to-grain attraction resulting from these forces should decrease in all

appearances with the size of the water bridge. This interpretation would lead to conclude that the resultant of suction stress (and shear strength) should prove lower on the desorption-sorption path than its counterpart on the desorption path at the same matric suction. Yet, the opposite is observed!

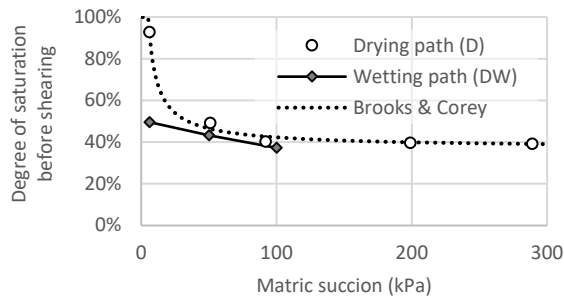


Fig. 7. Degree of saturation of triaxial specimens at equilibrium (before shearing) after desorption (drying path) and after desorption sorption (wetting path) under $(\sigma_3-u_a) = 100$ kPa.

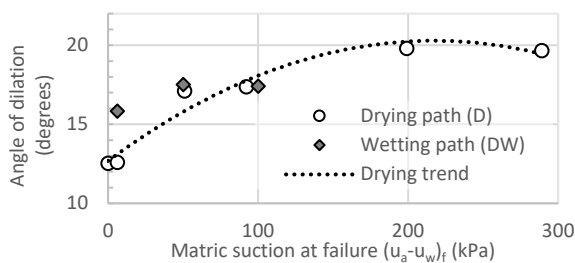


Fig. 8. Angles of dilation after desorption (D) and desorption sorption (DW) paths measured under $(\sigma_3-u_a)_x = 100$ kPa.

In consideration of the nature of the retention curve reported earlier, all unsaturated desorption tests in this study (except the one performed at 5 kPa matric suction after desorption) proceed at matric suctions above the residual value (Fig. 7). Those after desorption-sorption exceed or rest close to their water-entry value. According to [9], at such water contents “pore water exists in a pendular state of isolated pockets, thin films or as disconnected menisci among the soil grains.” In this regime, there exists practically no continuous network of the liquid phase, and the movement of water operates mainly by transport mechanisms in the gaseous phase.

In the axis-translation technique used for this study, desorption proceeds by reducing the water pressure at the base while maintaining the air pressure constant. This raises matric suction in the funicular (connected) water network. As this suction increases, the funicular regime fragments, leaving behind isolated water bridges in pendular regime. In these water bridges, the water would remain at the suction that led to their disconnection from the funicular regime. If time permits, however, the exchange of water vapour with the pore air would bring matric suction in all water bridges to equilibrate to the value imposed to the funicular network. In the triaxial tests carried out in this study (and in a practical loading), time prevented water vapour transport to establish this equilibrium.

The sorption stage leads to a gradual redevelopment of the funicular regime. However, the hysteresis effect impedes reconnection of all water bridges initially isolated during the desorption phase. As proof, as matric

suction decreases, water content on the sorption segment increases at a lower gradient and remains below its desorption counterpart (Figs. 2 and 7). Thus, a part of the water of the desorption curve that rested in the funicular regime doesn’t reappear in that of the sorption curve. At least not before reaching the water-entry value. As a result, many pendular water bridges created during the drying stage do not reconnect to the funicular regime while wetting. These pendular lenses would be inhabited by a matric suction equal to that attained at the time of pendular fragmentation from the funicular regime during drying. At the macroscale, suction stress corresponds to an average of the forces exerted in the funicular regime and those in the disconnected water bridges. Thus, at equal matric suctions, the average suction stress would be higher in the granular soil studied after a drying step followed by wetting than after drying alone. As a result, the material would prove more resistant for a given suction along a drying and wetting path than after drying alone. Provided, however, that wetting prevents the redeveloping funicular regime to reach all the isolated pendular water. For the tests after sorption of this study, this appears the case since shearing proceeds at water contents lower than the water-entry value. Furthermore, the duration of the equilibrium phase and the shearing rate of this study shouldn’t have been sufficient for the action of water vapour transport to establish equalization of matric suction inside the isolated water bridge with water in the funicular regime.

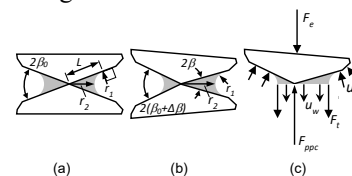


Fig. 9. Air-water-solid interaction for two angular particles: (a) symmetric opening angle $(2\beta_0)$ and principal radii of curvature r_1 and r_2 of contractile skin; (b) tilted $2\Delta\beta$ about the contact point $(\beta = \beta_0 - \Delta\beta)$; (c) free-body diagram of tilted particles (air pressure u_a , force due to surface tension of contractile skin F_s , water pressure u_w within water bridge, external force due to self-weight and loading F_e , particle to particle contact force F_{ppc}).

Like for saturated shear tests, the material in the unsaturated state should intuitively drain during the volume contraction phase and absorb water during the subsequent dilation phase. On the other hand, the contraction phase should decrease pore sizes thus raising capillary ascent and yield water absorption while the dilation phase should act inversely. Curiously, observations don’t agree with either reasoning. Drainage occurs during the first phase of contraction and pursues even so during the subsequent dilation phase (Fig. 3). This result initially appears as counterintuitive. However, the earlier described conceptual model can shed some light.

According to the Young-Laplace equation, matric suction (or Laplace pressure) is for an air-water interface contact angle of zero degree expressed by:

$$u_a - u_w = T_s \left(\frac{1}{r_1} - \frac{1}{r_2} \right) \quad (4)$$

Where T_s and r_1 and r_2 represent surface tension and principal radii of curvature of the air-water interface. For

the case of tilting angular particles, it proves rather complex to establish a relationship between r_1 and r_2 and opening angle β (Fig. 9b). However, it becomes possible to determine such a relationship if two bars of the same cross-section replace these grains. If they turn out sufficiently long, the radius of curvature r_2 tends towards infinity so that matric suction simplifies for practical purpose to:

$$u_a - u_w = T_s \frac{1}{r_1} \quad (5)$$

If the water on the right interconnects to the water on the left (for example by each end of the bars), matric suction will equalize on both sides. As a result, the radius r_1 will be the same on the right as on the left. It follows that r_1 can be expressed in function of the volume V_w of a water bridge and of the initial opening and tilted angles β_0 and β (Fig. 9a) as:

$$r_1 = \left[-2 \left((-1 + \tan(\beta)) (\pi - 2\beta_0) \right) \tan(\beta - 2\beta_0) + \tan(\beta) \right) \tan(\beta - 2\beta_0) \tan(\beta) V_w \right]^{0.5} / \{ [-1 + \tan(\beta) (\pi - 2\beta_0)] \tan(\beta - 2\beta_0) + \tan(\beta) \} \quad (6)$$

Matric suction for its part is inversely proportional to the latter as per equation (5).

Once a water bridge is disconnected from the funicular regime, its volume remains constant in consideration to the slow water vapour transport mechanism. As particles tilt one about one another during shear, geometry forces the contractile skin to reposition (Fig. 9b) and impose radius r_1 to decrease following (6). This brings matric suction to rise according to (5).

The fragmentation of the funicular regime by drying should leave behind pendular water that widely occupies all the opening illustrated in Fig. 9. Since length L increases as the inclination of both particles increases (Fig. 9b), shearing will squeeze the water on the tilting side towards the opening boundary. At this point, further slanting would lead to a discharge of the water bridge into the adjacent pore space. It could then interconnect with the funicular regime, adjust its matric suction to the latter and drain from the specimen. This could explain why shearing generates drainage.

Where the water bridge is well inside the boundaries of an opening such as illustrated in Fig. 9, tilting of two grains induced by shearing not only augments matric suction but also offsets the water bridge. This decreases r_1 , raising: suction stress, the resultant reaction force at their point of contact and the eccentricity of the latter (Fig. 9c). On the leaning side, reaction forces should increase on lateral points of contact with neighbouring particles (while relaxing on the opposite side). This intensifies friction and therefore shear resistance at these lateral points of contact. Grain groups where this phenomenon would occur could prove more solidary and exhibit a behaviour like a single deformable grain. Thus, shearing this structure would not only produce a relative movement between individual particles, but also between grain groups. This could explain why dilation rises with applied suction. In contrast, other tests (not presented) show that dilation decreases as confining stress increases. However, confinement doesn't create traction, hence no "capillary bonding" at points of contact. Under confining stress alone, the structure retains a single-grain character.

5 Conclusion

The following conclusions are drawn: (1) Specimens containing millimetre size voids cannot maintain saturation by capillarity and may possibly display a null air-entry value; (2) the size of a representative volume of material imposes a minimum experimentally achievable matric suction of not lower than 0.1 kPa; (3) the tested granular soil has an internal friction angle of 43.6° and a ϕ^b angle of 42.5° ; (4) the material behaves as a typical dense granular soil during shearing; (5) drying followed by wetting yields higher mechanical properties than after drying alone, hence revealing that hysteresis of water content comes with hysteresis of the latter; (6) proper modelling of granular materials requires to consider not only matric suction and net stress, but also the water content path, (7) shearing a pendular model of two bars making an angular opening at their point of contact shows that tilting induces changes in matric suction and gives insight on why the dilation phase comes with water drainage.

Acknowledgements: The Université de Moncton and the New Brunswick Innovation Foundation's (NBIF) STEM and Social Innovation Scholarship Fund provided funding for this study.

References

1. T. Nishimura and D. G. Fredlund, *Hysteresis effects resulting from drying and wetting under relatively dry conditions*, in Proceedings of the Third International Conference on Unsaturated Soils, UNSAT, Recife, Brazil, (2002), pp. 301–305.
2. C. N. Khoury and G. A. Miller, *Geotech. Test. J.*, **35**, 1, (2012), doi: 10.1520/GTJ103616.
3. K. H. Head, *Manual of soil laboratory testing: effective stress tests*, vol. 3. John Wiley & Sons, (1998).
4. C. W. W. Ng and Y. W. Pang, *J. Geotech. Geoenviron. Eng.*, **126**, 2, p. 157, (2000), doi: 10.1061/(ASCE)1090-0241(2000)126:2(157).
5. H. F. Zhao and L. M. Zhang, *Can. Geotech. J.*, **51**, 12, (2014), doi: 10.1139/cgj-2012-0292.
6. (J. W. Strutt) Lord Rayleigh, *Proceedings of the Royal Society of London. Series A, Containing Papers of a Mathematical and Physical Character*, **92**, 637, pp. 184–195, (1916), doi: 10.1098/rspa.1916.0004.
7. S. D. N. Lourenço, D. Gallipoli, C. E. Augarde, D. G. Toll, P. C. Fisher, and A. Congreve, *Géotechnique*, **62**, 3, pp. 193–199, (2012), doi: 10.1680/geot.11.P.034.
8. D. G. Fredlund, N. R. Morgenstern, and R. A. Widger, *Can. Geotech. J.*, **15**, 3, pp. 313–321, (1978), doi: 10.1139/t78-029.
9. N. Lu and W. J. Likos, *Unsaturated soil mechanics*. Hoboken, N.J: J. Wiley, (2004).
10. N. Lu and W. J. Likos, *J. Geotech. Geoenviron. Eng.*, vol. 132, no. 2, pp. 131–142, (2006), doi: 10.1061/(ASCE)1090-0241(2006)132:2(131).